MPHYS Project

Early Universe Resonances:

Preheating of Light Bosons and Heavy Fermions

Ana Alexandre

The University of Manchester

May 23, 2020

- Inflation is a period of exponential expansion in the Early Universe

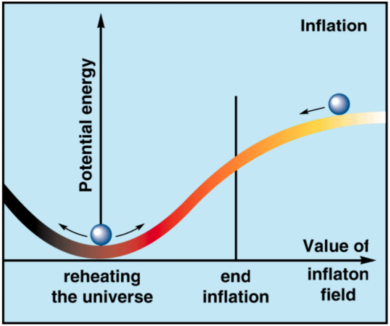

Figure: Inflaton field as a ball rolling down to its minimum (García-Bellido, 1999)

- Inflation is a period of exponential expansion in the Early Universe
- During inflation, the Universe is occupied by the inflaton field ϕ

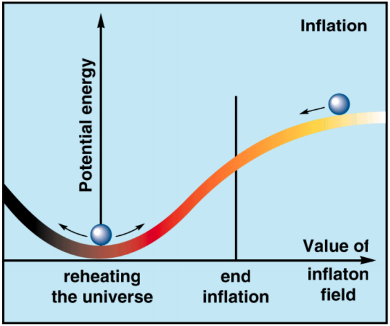

Figure: Inflaton field as a ball rolling down to its minimum (García-Bellido, 1999)

- Inflation is a period of exponential expansion in the Early Universe
- During inflation, the Universe is occupied by the inflaton field ϕ
- Inflation is followed by the period of reheating where most of the matter that makes up the universe today was created

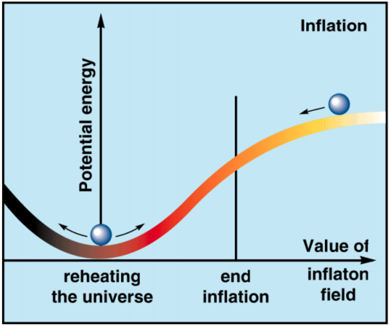

Figure: Inflaton field as a ball rolling down to its minimum (García-Bellido, 1999)

- First stage of reheating
- The inflaton field ϕ rolls down its potential and oscillates around its minimum

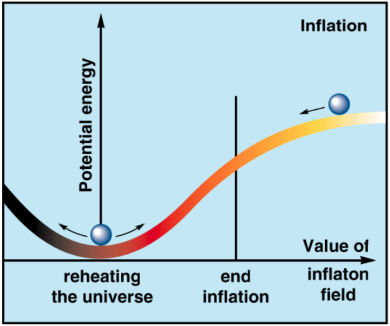

Figure: Inflaton field as a ball rolling down to its minimum (García-Bellido, 1999)

- First stage of reheating
- The inflaton field ϕ rolls down its potential and oscillates around its minimum
- As it oscillates, it can transfer its energy to create new particles

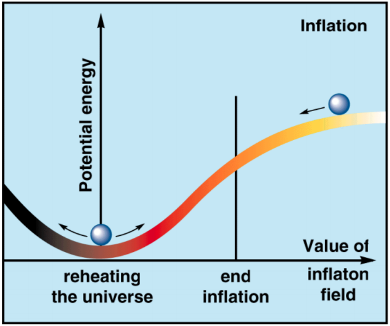

Figure: Inflaton field as a ball rolling down to its minimum (García-Bellido, 1999)

Why Study Preheating?

- Could increase our understanding of inflation in the context of Particle Physics

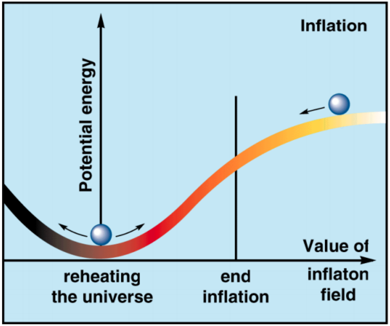

Figure: Inflaton field as a ball rolling down to its minimum (García-Bellido, 1999)

Why Study Preheating?

- Could increase our understanding of inflation in the context of Particle Physics

- Possibility to produce heavy particles, with masses much larger than the inflaton, about $10^{13} - 10^{17}\mathrm{GeV}$, even when single particle decay is forbidden

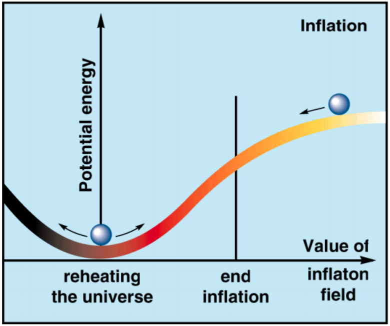

Figure: Inflaton field as a ball rolling down to its minimum (García-Bellido, 1999)

Why Study Preheating?

- It could be applied to a variety of cosmological contexts

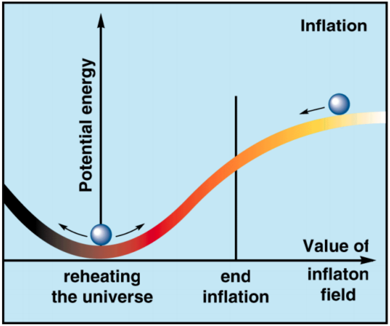

Figure: Inflaton field as a ball rolling down to its minimum (García-Bellido, 1999)

Why Study Preheating?

- It could be applied to a variety of cosmological contexts
- Provides a possible explanation for the origin of Baryon Asymmetry

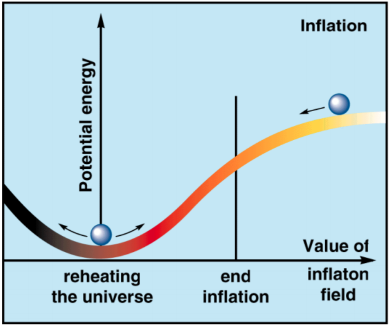

Figure: Inflaton field as a ball rolling down to its minimum (García-Bellido, 1999)

Why Study Preheating?

- It could be applied to a variety of cosmological contexts
- Provides a possible explanation for the origin of Baryon Asymmetry
- Provides a possible method to create super-heavy fermionic Dark Matter

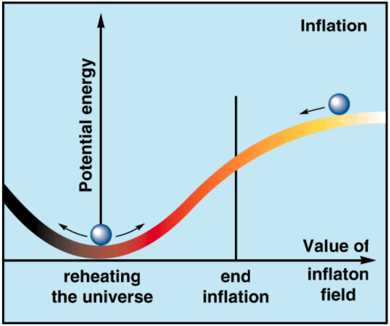

Figure: Inflaton field as a ball rolling down to its minimum (García-Bellido, 1999)

Inflaton Potential

$$V(\phi) = \frac{1}{2} m_\phi^2 \phi^2$$

where

- ϕ is the (scalar) inflaton field
- $m_\phi \simeq 10^{13}\mathrm{GeV}$

The Inflaton Field
Basic Formalism of Preheating

An expanding Universe containing an homogeneous scalar field such as ϕ can be described by

$$H^2 = \frac{8\pi}{3M_{Pl}^2}\left[V(\phi) + \frac{1}{2}\dot{\phi}^2\right],$$
$$\ddot{\phi} + 3H\dot{\phi} + \frac{dV(\phi)}{d\phi} = 0. \tag{1}$$

An expanding Universe containing an homogeneous scalar field such as ϕ can be described by

$$H^2 = \frac{8\pi}{3M_{Pl}^2}\left[V(\phi) + \frac{1}{2}\dot{\phi}^2\right], \qquad (1)$$
$$\ddot{\phi} + 3H\dot{\phi} + \frac{dV(\phi)}{d\phi} = 0.$$

Using the quadratic inflaton potential,

$$a \propto \eta^2$$
$$t \propto a^{3/2}$$

where conformal time η is defined as $d\eta = \frac{dt}{a}$

Without taking into account the backreaction of created particles,

$$\phi(t) \simeq \phi_0(t)\cos(m_\phi t)$$

Without taking into account the backreaction of created particles,

$$\phi(t) \simeq \phi_0(t)\cos(m_\phi t)$$

- In a static Universe, with $a = 1$,

$$\phi(t) \simeq \phi_0(t_0)\cos(m_\phi t)$$

Without taking into account the backreaction of created particles,

$$\phi(t) \simeq \phi_0(t)\cos(m_\phi t)$$

- In a static Universe, with $a = 1$,

$$\phi(t) \simeq \phi_0(t_0)\cos(m_\phi t)$$

- In an expanding Universe, with $a \propto \eta^2$,

$$\phi(t) \simeq \frac{M_{Pl}}{\sqrt{3\pi}} \frac{\cos(m_\phi t)}{m_\phi t}$$

The interaction Lagrangian between the inflaton field $\phi(t)$ and the massive Boson fields $\varphi(x)$

$$\mathcal{L}_\varphi = \frac{1}{2}(\partial_\mu \varphi)^2 - \frac{m_\varphi^2}{2}\varphi^2 - \frac{1}{2} g \phi(t) \varphi^2$$

The interaction Lagrangian between the inflaton field $\phi(t)$ and the massive Boson fields $\varphi(x)$

$$\mathcal{L}_\varphi = \frac{1}{2}(\partial_\mu \varphi)^2 - \frac{m_\varphi^2}{2}\varphi^2 - \frac{1}{2} g \phi(t) \varphi^2$$

This gives the differential equation

$$\ddot{\varphi}_k + \omega_k^2(t) \varphi_k = 0$$

where $\omega_k^2(t) = k^2 + M_\varphi^2 + g^2 \phi^2(t)$ and $M_\varphi \ll m_\phi$

A general solution is

$$\varphi_k(t) = \varphi_k^+(t)A_k^\dagger + \varphi_k^-(t)A_{-k}$$

where $A_k^{(\dagger)}$ are creation/destruction operators with $A_k\,|0_{\rm in}\rangle = 0$.

A general solution is

$$\varphi_k(t) = \varphi_k^+(t)A_k^\dagger + \varphi_k^-(t)A_{-k}$$

where $A_k^{(\dagger)}$ are creation/destruction operators with $A_k\,|0_{\rm in}\rangle = 0$.

In terms of the final solutions and creation/destruction operators $\widetilde{\varphi}_k^\pm$ and $\widetilde{A}_k^{(\dagger)}$,

$$\varphi_k(t) = \widetilde{\varphi}_k^+(t)\widetilde{A}_k^\dagger + \widetilde{\varphi}_k^-(t)\widetilde{A}_{-k}$$

- The initial and final creation and destruction operators are linearly related.

- The initial and final creation and destruction operators are linearly related.

Bogolyubov Transformation

$$\widetilde{A}_k^\dagger = \alpha_k A_k^\dagger + \beta_k A_{-k}, \\ \widetilde{A}_k = \alpha_k^* A_k + \beta_k^* A_{-k}^\dagger. \tag{2}$$

- The initial and final creation and destruction operators are linearly related.

Bogolyubov Transformation

$$\widetilde{A}_k^\dagger = \alpha_k A_k^\dagger + \beta_k A_{-k}, \qquad (2)$$
$$\widetilde{A}_k = \alpha_k^* A_k + \beta_k^* A_{-k}^\dagger.$$

- The Bogolyubov coefficients α_k and β_k obey

$$|\alpha_k(\eta)|^2 - |\beta_k(\eta)|^2 = 1$$

- The initial and final creation and destruction operators are linearly related.

Bogolyubov Transformation

$$\widetilde{A}_k^\dagger = \alpha_k A_k^\dagger + \beta_k A_{-k},$$
$$\widetilde{A}_k = \alpha_k^* A_k + \beta_k^* A_{-k}^\dagger. \tag{2}$$

- The Bogolyubov coefficients α_k and β_k obey

$$|\alpha_k(\eta)|^2 - |\beta_k(\eta)|^2 = 1$$

- We can define the number operator at time t

$$n_k = \widetilde{A}_k^\dagger \widetilde{A}_k = |\beta_k|^2$$

The equation of motion can be written as the Mathieu Equation

Mathieu Equation

$$\ddot{\theta} + (A + 2q\cos(2\tau))\theta = 0$$

The equation of motion can be written as the Mathieu Equation

Mathieu Equation

$$\ddot{\theta} + (A + 2q\cos(2\tau))\theta = 0$$

with the non-dimensional parameters A, q and τ defined as

$$\begin{aligned} A &= \frac{k^2}{m_\phi^2} + 2q, \\ q &= \frac{g^2\phi_0^2}{4m_\phi^2}, \\ \tau &= m_\phi t. \end{aligned} \tag{3}$$

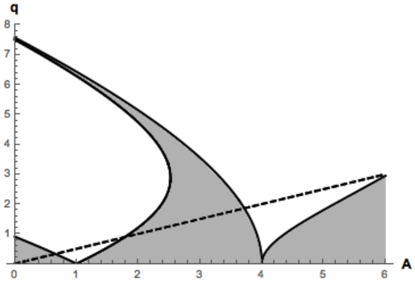

Figure: Resonance regions of the Mathieu equation. Dashed line: $A = 2q$.

If $g\phi_0 < m_\phi$ $(q \ll 1)$

- Narrow resonance regime

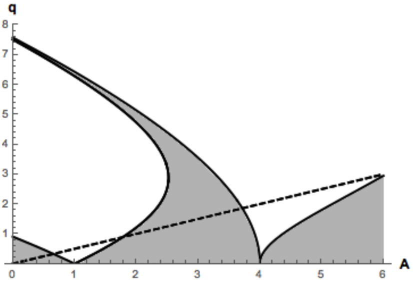

Figure: Resonance regions of the Mathieu equation. Dashed line: $A = 2q$.

If $g\phi_0 < m_\phi$ ($q \ll 1$)

- Narrow resonance regime

Different parameter regions:

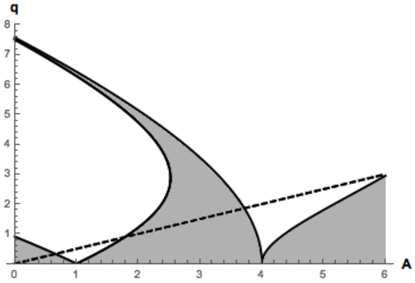

Figure: Resonance regions of the Mathieu equation. Dashed line: $A = 2q$.

If $g\phi_0 < m_\phi$ ($q \ll 1$)

- Narrow resonance regime

Different parameter regions:

- Regions of instability (white regions):

- Regions of stability (grey regions):

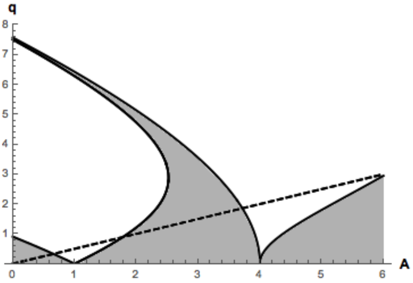

Figure: Resonance regions of the Mathieu equation. Dashed line: $A = 2q$.

If $g\phi_0 < m_\phi$ $(q \ll 1)$

- Narrow resonance regime

Different parameter regions:

- Regions of instability (white regions):
  - Exponential growth
- Regions of stability (grey regions):
  - Quasi-periodic oscillations

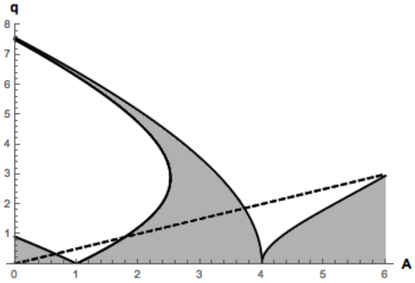

Figure: Resonance regions of the Mathieu equation. Dashed line: $A = 2q$.

If $g\phi_0 > 2m_\phi$ ($q \gg 1$)

- Broad resonance regime

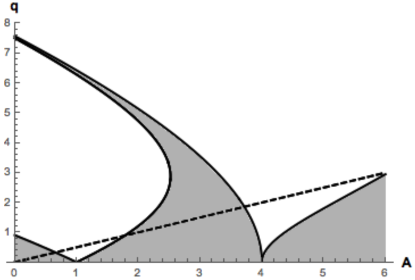

Figure: Resonance regions of the Mathieu equation. Dashed line: $A = 2q$.

If $g\phi_0 > 2m_\phi$ ($q \gg 1$)

- Broad resonance regime
- Particle production can be very efficient if evolution of $\omega_k(t)$ is not adiabatic

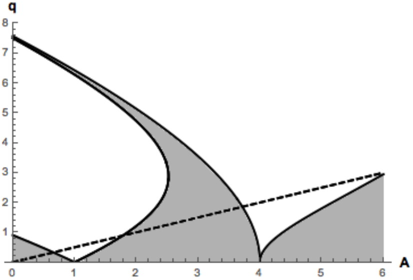

Figure: Resonance regions of the Mathieu equation. Dashed line: $A = 2q$.

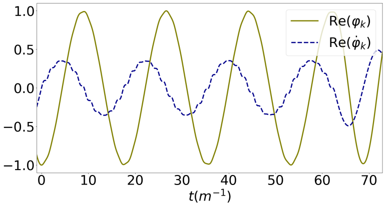

Figure: $\mathrm{Re}(\varphi_k)$ and $\mathrm{Re}(\dot{\varphi}_k)$ against time t for $q = 1/64$: the amplitude oscillates (quasi) periodically

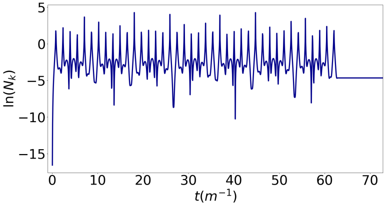

Figure: $\ln n_k$ against time t for $q = 1/64$: no particles are created

Narrow Resonance – Unstable Region

Boson Numerical Results

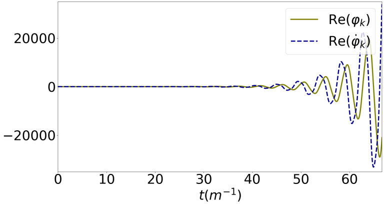

Figure: Re(φ_k) and Re($\dot{\varphi}_k$) against time t for $q = 1/2$: the amplitude grows exponentially with time

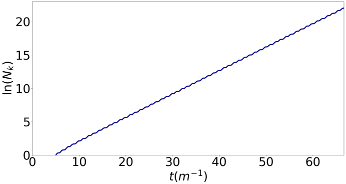

Figure: $\ln n_k$ against time t for $q = 1/2$: the number of particles also grows exponentially with time

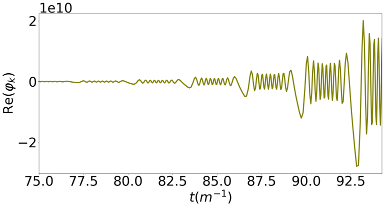

Figure: Re(φ_k) and Re($\dot{\varphi}_k$) against time t for $q = 200$: the field's amplitude grows exponentially in small time intervals

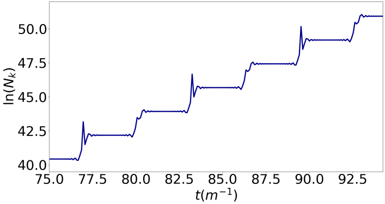

Figure: ln n_k against time t for $q = 200$: the number of particles created grows exponentially the same time intervals and remains constant otherwise

Resonance Spectrum
Boson Numerical Results

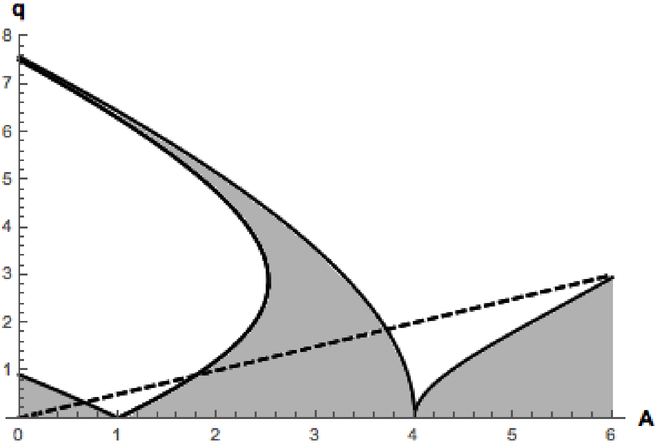

Figure: Resonance regions of the Mathieu equation. Dashed line: $A = 2q$.

- The first resonance band is the only in the narrow resonance regime.

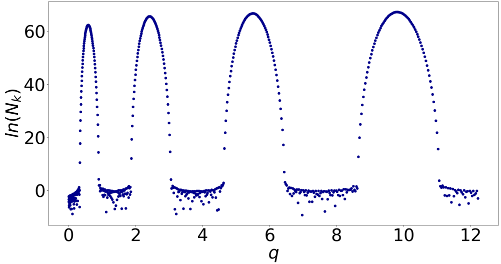

Figure: Plot of $\ln n_k$ against q along the line $A = 2q$, where $k = 0$, showing the structure of the resonance bands of the Mathieu equation.

- The first resonance band is the only in the narrow resonance regime.
- Others bands belong to the broad resonance regime.

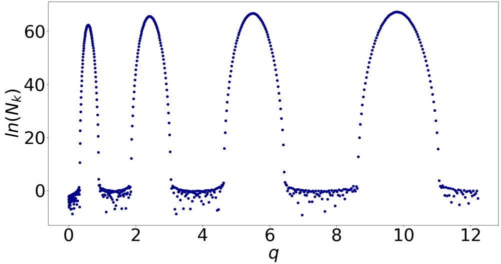

Figure: Plot of $\ln n_k$ against q along the line $A = 2q$, where $k = 0$, showing the structure of the resonance bands of the Mathieu equation.

- The first resonance band is the only in the narrow resonance regime.
- Others bands belong to the broad resonance regime.
- Consistent with previous simulations in Kofman, Linde, and Starobinsky 1997

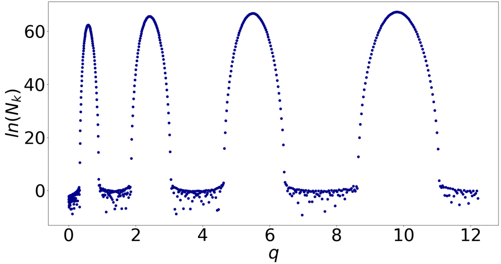

Figure: Plot of $\ln n_k$ against q along the line $A = 2q$, where $k = 0$, showing the structure of the resonance bands of the Mathieu equation.

Conclusions: Bosons

- Production of light bosons was analysed for a quadratic inflaton potential in a static Universe.

Conclusions: Bosons

- Production of light bosons was analysed for a quadratic inflaton potential in a static Universe.
- Particle production exhibits parametric resonance following the Mathieu equation.

Conclusions: Bosons

- Production of light bosons was analysed for a quadratic inflaton potential in a static Universe.
- Particle production exhibits parametric resonance following the Mathieu equation.
- Different combinations of g, q and ϕ_0 lead to different parameter regions: stable or unstable.

Conclusions: Bosons

- Production of light bosons was analysed for a quadratic inflaton potential in a static Universe.
- Particle production exhibits parametric resonance following the Mathieu equation.
- Different combinations of g, q and ϕ_0 lead to different parameter regions: stable or unstable.
- The behaviour of the system is consistent with previous simulations Kofman, Linde, and Starobinsky 1997.

The inflaton field ϕ couples to the Dirac Fermions X through the Yukawa coupling

$$\mathcal{L}_Y = g\phi\bar{X}X$$

where

- g is the coupling constant

Total fermionic mass

$$M(t) = M_X + g\phi(t)$$

where

- M_X is the bare fermion mass

Total fermionic mass

$$M(t) = M_X + g\phi(t)$$

where

- M_X is the bare fermion mass

- Fermion production occurs whenever evolution of M(t) is non-adiabatic
- Satisfied when $M(t) \simeq 0$, i.e. $|\phi(t)| = M_X/g$

Dirac Equation for the fermion field X with the FRW metric

$$\left(\frac{i}{a}\gamma^{\mu}\partial_{\mu} + \frac{3}{2}H\gamma^{0} - M\right)X = 0$$

Dirac Equation for the fermion field X with the FRW metric

$$\left(\frac{i}{a}\gamma^{\mu}\partial_{\mu} + \frac{3}{2}H\gamma^{0} - M\right)X = 0$$

which can be written as

$$(i\gamma^{\mu}\partial_{\mu} - aM)\chi = 0$$

where $\chi = a^{3/2}X$.

Quantization of χ

$$\chi(x) = \int \frac{d^3k}{(2\pi)^{3/2}} e^{-i\mathbf{k}\cdot\mathbf{x}} \sum_s \Big(u_s(\eta, k) a_s(k) + v_s(\eta, k) b_s^\dagger(-k) \Big)$$

where

- $b_s^{(\dagger)}$ and $a_s^{(\dagger)}$ are creation and destruction operators
- $s = +, -$ has two possible spin values
- u_s and v_s are Dirac spinors

Normalising the spinors such that

$$u_s = \begin{pmatrix} \frac{u_+}{\sqrt{2}}\psi_s \\ \frac{u_-}{\sqrt{2}}\psi_s \end{pmatrix} \qquad v_s = \begin{pmatrix} \frac{v_+}{\sqrt{2}}\psi_s \\ \frac{v_-}{\sqrt{2}}\psi_s \end{pmatrix}$$

Normalising the spinors such that

$$u_s = \begin{pmatrix} \frac{u_+}{\sqrt{2}}\psi_s \\ \frac{u_-}{\sqrt{2}}\psi_s \end{pmatrix} \qquad v_s = \begin{pmatrix} \frac{v_+}{\sqrt{2}}\psi_s \\ \frac{v_-}{\sqrt{2}}\psi_s \end{pmatrix}$$

The equations of motion can be derived

Equations of Motion

$$u'_\pm(\eta) = iku_\mp(\eta) \mp iaMu_\pm(\eta) \tag{4}$$

$$u''_\pm + \left[\omega_k^2 \pm i(Ma)'\right] u_\pm = 0 \tag{5}$$

where $\omega_k^2 = k^2 + a^2M^2$

- It is possible to calculate the number of created particles at time η by performing a Bogolyubov transformation

- It is possible to calculate the number of created particles at time η by performing a Bogolyubov transformation
- The Bogolyubov coefficients α_k and β_k obey

$$|\alpha_k(\eta)|^2 + |\beta_k(\eta)|^2 = 1 \tag{6}$$

- It is possible to calculate the number of created particles at time η by performing a Bogolyubov transformation

- The Bogolyubov coefficients α_k and β_k obey

$$|\alpha_k(\eta)|^2 + |\beta_k(\eta)|^2 = 1 \quad (6)$$

- The number operator at time η is given by $n_k = |\beta_k|^2$

Fermion Numerical Results

- Equation (4) was numerically solved

Fermion Numerical Results

- Equation (4) was numerically solved
- To compare with the bosonic case, we can define a parameter q as

$$q \equiv \frac{g^2 \phi(\eta_0)^2}{4 m_\phi^2}$$

- Fermions are created through parametric resonance blocked by the Pauli Principle

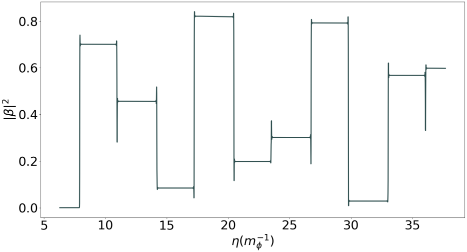

Figure: Plot of $|\beta_k|^2$ against η, given in units of m_ϕ^{-1}, for $q = 10^6$, $M_X = 100 m_\phi$ and $N = 5$ inflaton oscillations.

- Fermions are created through parametric resonance blocked by the Pauli Principle
- n_k jumps sharply between 0 and 1 during short intervals where $M(t) \simeq 0$ and remains constant otherwise

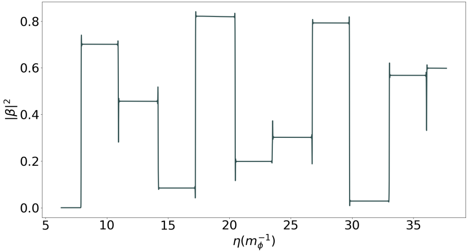

Figure: Plot of $|\beta_k|^2$ against η, given in units of m_ϕ^{-1}, for $q = 10^6$, $M_X = 100 m_\phi$ and $N = 5$ inflaton oscillations.

- Fermions are created through parametric resonance blocked by the Pauli Principle

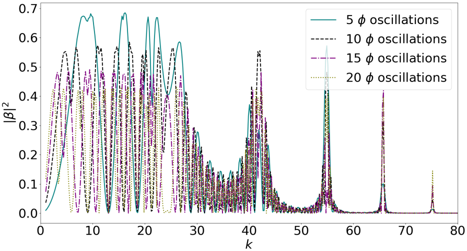

Figure: Plot of $|\beta_k|^2$ against k, for $q = 10^6$ and $M_X = 100 m_\phi$, for a different number of completed inflaton field oscillations, $N = 5, 10, 15, 20$.

- Fermions are created through parametric resonance blocked by the Pauli Principle
- The first resonance band is the broadest one, with the bandwidth lowering as k increases

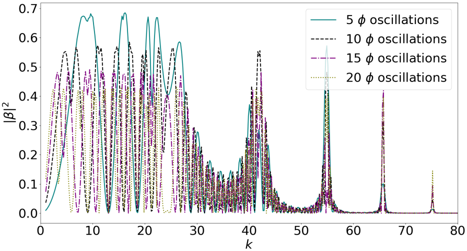

Figure: Plot of $|\beta_k|^2$ against k, for $q = 10^6$ and $M_X = 100m_\phi$, for a different number of completed inflaton field oscillations, $N = 5, 10, 15, 20$.

- Including the expansion of the Universe will destroy the clear parametric-resonance picture

- Including the expansion of the Universe will destroy the clear parametric-resonance picture

- It allows for the occupation of modes that were previously forbidden making the production of fermions more effective

- The creation of fermions occurs up to a maximum co-moving momentum, $k_{\max}$, where the Fermi distribution becomes saturated

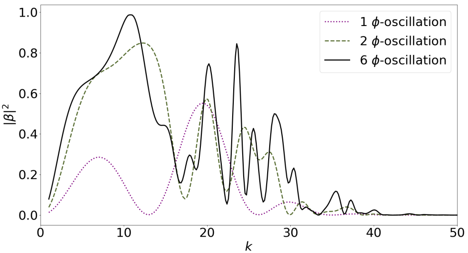

Figure: Plot of $|\beta_k|^2$ against k, for $q = 10^5$ and $M_X = 100m_\phi$, for $N = 1, 2, 6$ completed inflaton oscillations, with expansion taken into account.

Preheating in an Expanding Universe

Fermion Numerical Results

- The creation of fermions occurs up to a maximum co-moving momentum, $k_{\max}$, where the Fermi distribution becomes saturated
- At $k > k_{\max}$, particle production quickly drops to zero

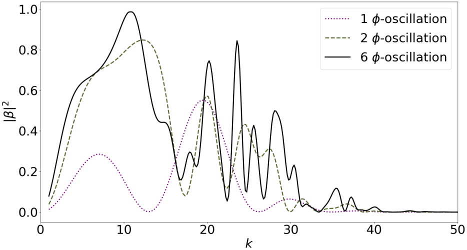

Figure: Plot of $|\beta_k|^2$ against k, for $q = 10^5$ and $M_X = 100 m_\phi$, for $N = 1, 2, 6$ completed inflaton oscillations, with expansion taken into account.

- The creation of fermions occurs up to a maximum co-moving momentum, $k_{\max}$, where the Fermi distribution becomes saturated
- At $k > k_{\max}$, particle production quickly drops to zero
- As the number of completed inflaton oscillations increases, so does the value of $k_{\max}$

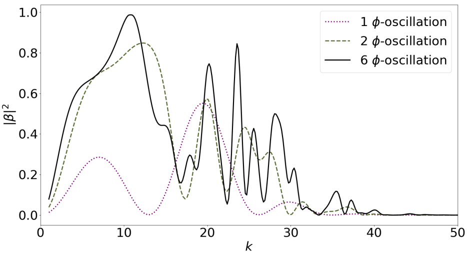

Figure: Plot of $|\beta_k|^2$ against k, for $q = 10^5$ and $M_X = 100m_\phi$, for $N = 1, 2, 6$ completed inflaton oscillations, with expansion taken into account.

- This occurs until particle production stops and the distribution of $|\beta_k|^2$ remains relatively constant with N

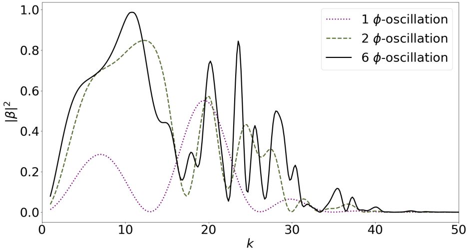

Figure: Plot of $|\beta_k|^2$ against k, for $q = 10^5$ and $M_X = 100m_\phi$, for $N = 1, 2, 6$ completed inflaton oscillations, with expansion taken into account.

- This occurs until particle production stops and the distribution of $|\beta_k|^2$ remains relatively constant with N
- The number of oscillations it is required to reach the final distribution depends on the value of q

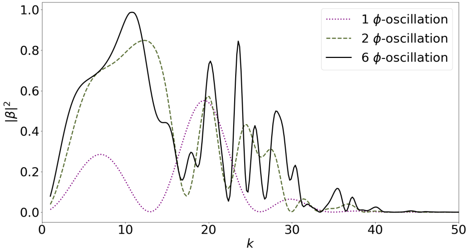

Figure: Plot of $|\beta_k|^2$ against k, for $q = 10^5$ and $M_X = 100m_\phi$, for $N = 1, 2, 6$ completed inflaton oscillations, with expansion taken into account.

- This occurs until particle production stops and the distribution of $|\beta_k|^2$ remains relatively constant with N
- The number of oscillations it is required to reach the final distribution depends on the value of q
- For $q = 10^5$, $N = 6$ corresponds to the final distribution.

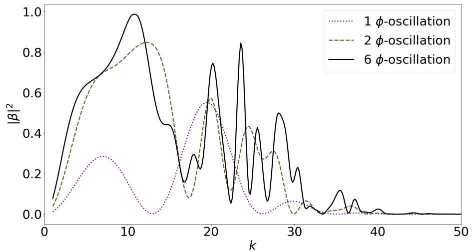

Figure: Plot of $|\beta_k|^2$ against k, for $q = 10^5$ and $M_X = 100m_\phi$, for $N = 1, 2, 6$ completed inflaton oscillations, with expansion taken into account.

- n_k jumps sharply between 0 and 1 during short intervals where $M(t) \simeq 0$ until particle production stops

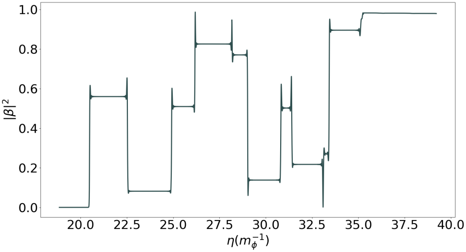

Figure: Plot of $|\beta_k|^2$ against η, in units of m_ϕ^{-1}, for $q = 10^5$, $M_X = 100m_\phi$ and $N = 8$, with expansion taken into account.

Preheating in an Expanding Universe

Fermion Numerical Results

- n_k jumps sharply between 0 and 1 during short intervals where $M(t) \simeq 0$ until particle production stops
- Particle production ends after the 6th oscillation and n_k remains constant

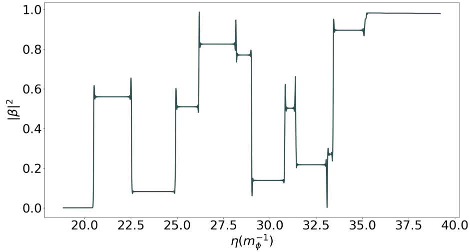

Figure: Plot of $|\beta_k|^2$ against η, in units of m_ϕ^{-1}, for $q = 10^5$, $M_X = 100 m_\phi$ and $N = 8$, with expansion taken into account.

- Final distributions for $q = 10^3, 10^4, 10^5, 10^6$

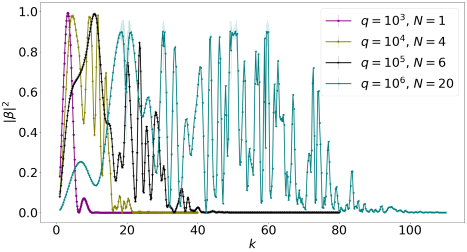

Figure: Plot of the final distributions of $|\beta_k|^2$ against k, for $q = 10^3, 10^4, 10^5, 10^6$ and $M_X = 30, 40, 100, 100 m_\phi$.

- Final distributions for $q = 10^3, 10^4, 10^5, 10^6$
- The number of oscillations required to reach the final distribution was, respectively, $N = 1, 4, 6, 20$

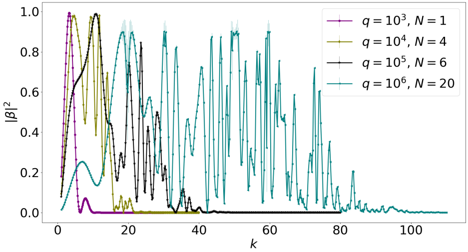

Figure: Plot of the final distributions of $|\beta_k|^2$ against k, for $q = 10^3, 10^4, 10^5, 10^6$ and $M_X = 30, 40, 100, 100 m_\phi$.

- Final distributions for $q = 10^3, 10^4, 10^5, 10^6$
- The number of oscillations required to reach the final distribution was, respectively, $N = 1, 4, 6, 20$
- k_{max} increases with q

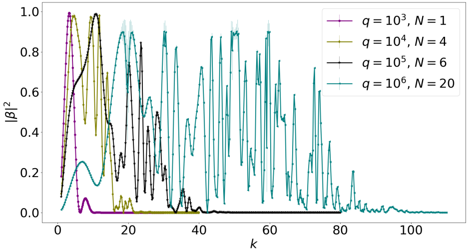

Figure: Plot of the final distributions of $|\beta_k|^2$ against k, for $q = 10^3, 10^4, 10^5, 10^6$ and $M_X = 30, 40, 100, 100 m_\phi$.

- Final distributions for $q = 10^3, 10^4, 10^5, 10^6$
- The number of oscillations required to reach the final distribution was, respectively, $N = 1, 4, 6, 20$
- $k_{\max}$ increases with q
- Particle production is more effective for higher values of q

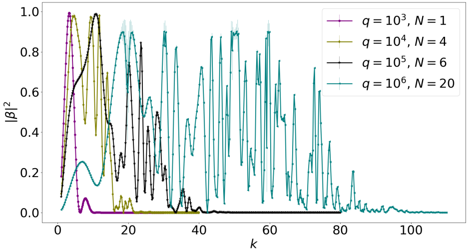

Figure: Plot of the final distributions of $|\beta_k|^2$ against k, for $q = 10^3, 10^4, 10^5, 10^6$ and $M_X = 30, 40, 100, 100 m_\phi$.

Conclusions: Fermions

- Production of spin-$1/2$ fermions was analysed for a quadratic inflaton potential in both a static and an expanding Universe.

Conclusions: Fermions

- Production of spin-$1/2$ fermions was analysed for a quadratic inflaton potential in both a static and an expanding Universe.

- Particle production occurs only in short intervals where $M(t) \simeq 0$ and remains constant otherwise.

Conclusions: Fermions

- Production of spin-$1/2$ fermions was analysed for a quadratic inflaton potential in both a static and an expanding Universe.

- Particle production occurs only in short intervals where $M(t) \simeq 0$ and remains constant otherwise.

- In a static Universe, parametric resonance was observed.

Conclusions: Fermions

- Production of spin-$1/2$ fermions was analysed for a quadratic inflaton potential in both a static and an expanding Universe.
- Particle production occurs only in short intervals where $M(t) \simeq 0$ and remains constant otherwise.
- In a static Universe, parametric resonance was observed.
- In an expanding Universe, production occurs up to a value $k_{\max}$, which increases with the number of total oscillations of the inflaton field until the ratio ρ_X/ρ_ϕ is saturated.

Possible Further Work

- Estimate analytical solutions in order to obtain faster simulations

Possible Further Work

- Estimate analytical solutions in order to obtain faster simulations
- Simulate preheating for different inflaton potentials

Possible Further Work

- Estimate analytical solutions in order to obtain faster simulations
- Simulate preheating for different inflaton potentials
- Apply these results to different cosmological contexts

Giudice, G.F. et al. (1999). “Production of Massive Fermions at Preheating and Leptogenesis”. In: *JHEP* 9908.014. URL: https://arxiv.org/abs/hep-ph/9905242.

Gorbunov, D. S. and V. A. Rubakov (2011). *Introduction to the Theory of the Early Universe: Cosmological Perturbations and Inflationary Theory*. World Scientific.

Greene, P. B. and L. Kofman (2000). “On the Theory of Fermionic Preheating”. In: *Phys. Lett. D* 62.123516.

Kofman, L., A. Linde, and A. Starobinsky (1997). “Towards the Theory of Reheating After Inflation”. In: *Phys Rev D56*, pp. 3258–3295. URL: https://arxiv.org/abs/hep-ph/9704452.

Peloso, M. and L. Sorbo (2000). “Preheating of massive fermions after inflation: analytical results”. In: *JHEP* 05.016.

Thank you for listening!

Any questions?

- For non-adiabatic evolution, must satisfy:

$$\left|\frac{\dot{\omega}_k}{\omega_k^2}\right| \lesssim \left|\frac{m_\phi}{g\phi_0}\frac{\sin(m_\phi t)}{\cos^2(m_\phi t)}\right|$$

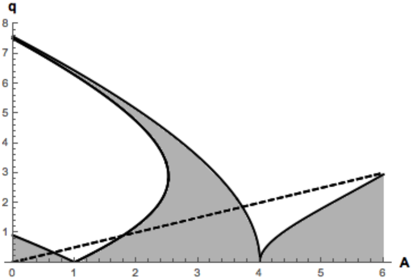

Figure: Resonance regions of the Mathieu equation. Dashed line: $A = 2q$.

- For non-adiabatic evolution, must satisfy:

$$\left|\frac{\dot{\omega}_k}{\omega_k^2}\right| \lesssim \left|\frac{m_\phi}{g\phi_0}\frac{\sin(m_\phi t)}{\cos^2(m_\phi t)}\right|$$

- Only true in small time intervals where $\phi(t) = 0$

$$t_n = (\pi/2 + \pi n)/m_\phi, n \in \mathbb{N}$$

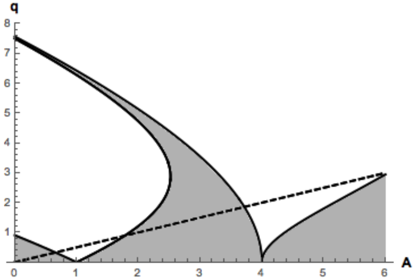

Figure: Resonance regions of the Mathieu equation. Dashed line: $A = 2q$.

Boson Numerical Results

- Goal is to numerically study the equation

$$\ddot{\varphi}_k + \omega_k^2(t)\varphi_k = 0$$

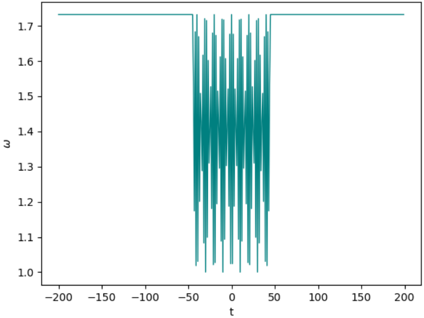

Figure: Example of the frequency, $\omega_k(t)$, of the system.

Hamiltonian

$$H(\eta) = \frac{1}{a}\int d^3k \sum_s \{E_k(\eta)[a_s^\dagger(k)a_s(k) - b_s(k)b_s^\dagger(k)] +$$
$$+F_k(\eta)b_s(-k)a_s(k) + F_k^*(\eta)a_s^\dagger(k)b_s^\dagger(-k)\}$$

where

$$E_k(\eta) = k\mathrm{Re}(u_+^* u_-) + aM(1 - u_+^* u_+)$$
$$F_k(\eta) = \frac{k}{2}(u_+^2 - u_-^2) + aMu_+u_-$$
$$E_k^2 + |F_k|^2 = \omega_k^2 \tag{7}$$

- It is possible to calculate the number of created particles at time η by performing a Bogolyubov transformation
- The Bogolyubov coefficients α_k and β_k obey

$$|\alpha_k(\eta)|^2 + |\beta_k(\eta)|^2 = 1 \tag{8}$$

and can be calculated as

$$\alpha_k(\eta) = \beta\left(\frac{E_k(\eta) + \omega(\eta)}{F_k^*(\eta)}\right)$$

$$|\beta_k(\eta)|^2 = \frac{|F_k(\eta)|^2}{2\omega(\eta)(E_k(\eta) + \omega(\eta))} = \frac{\omega(\eta) - E_k(\eta)}{2\omega(\eta)}$$

The density of created fermions can be calculated as

Particle density

$$n(\eta) = \langle 0 | \frac{n}{V} | 0 \rangle = \frac{1}{\pi^2 a^3} \int dk k^2 |\beta_k|^2$$

The energy density of the created fermions with respect to the inflaton energy density can be calculated as

Energy density

$$\frac{\rho_X}{\rho_\phi} = \frac{2M_X}{\pi^2} \int dk k^2 n_k \frac{2}{m_\phi^2 \phi_0^2}$$

- The period of the oscillations, in terms of the period of the inflaton oscillations $T_\phi = 2\pi$ decreases with N
- Suggests a linear relation $T_{|\beta_k|^2} \simeq -0.5N + 15$
- More N values must be studied for a more accurate fit

N	No. Peaks	$T_{\|\beta_k\|^2}(T_\phi)$
5	5	15 ± 3
10	9	11 ± 2
15	14	7.5 ± 1.5
20	21	5.6 ± 1.2

Table: Number of peaks and period of $|\beta_k|^2$ oscillations, $T_{|\beta_k|^2}$, for different N, in the first resonance band. The period ois given in terms of the period of the inflaton oscillations $T_\phi = 2\pi$.

- Once M_X is above a certain $M_X^{\max}$, the ratio ρ_X/ρ_ϕ is saturated and production no longer occurs
- The energy density exhibits small fluctuations around an average function
- The value of $M_X^{\max}$ increases with q

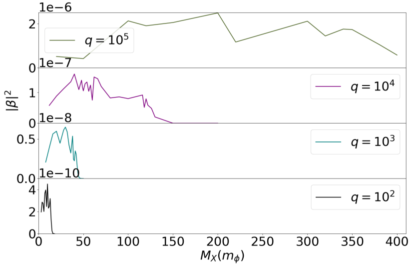

Figure: Plot of the final energy density of the created fermions ρ_X/ρ_ϕ against M_X for $q = 10^2, 10^3, 10^4, 10^5$.

For the approximated inflaton field, $M_X^{\max}$ can be estimated as

$$M_X^{\max} \simeq \frac{2\sqrt{q}}{\pi} m_\phi \tag{9}$$

For numerically determined the inflaton field in Giudice et al. 1999; Peloso and Sorbo 2000,

$$M_X^{\max} \simeq \frac{\sqrt{q}}{2} m_\phi \tag{10}$$

- The filled line shows the prediction (10) from Giudice et al. 1999
- The dashed line shows the linear regression of the data points with a slope of 0.475 ± 0.007
- This slope is consistent with the expected scaling of $M_X^{\max}$ with $\sqrt{q}$

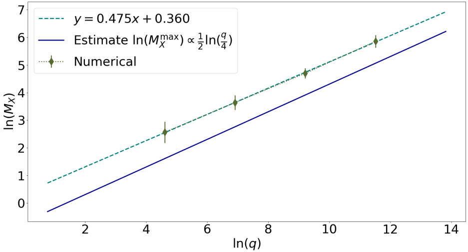

Figure: Plot of $\ln(M_X^{\max})$ against $\ln(q)$ for $q = 10^2, 10^3, 10^4, 10^5$.

- A systematic shift of the results can be observed, which is attributed to the combination of two effects:
  - the filled line corresponds to (10) but the simulations used the approximation of the inflaton field
  - the definition of $\phi(\eta_0)$ differs from what was used in Giudice et al. 1999

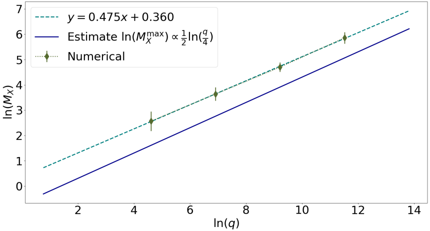

Figure: Plot of $\ln(M_X^{\max})$ against $\ln(q)$ for $q = 10^2, 10^3, 10^4, 10^5$.

There are several different estimates of k_{max} found in the literature

The estimate found in Giudice et al. 1999 is

$$k_{\mathrm{max}} = \left(2m_{\phi}^{4}\frac{q}{M_X}\right)^{1/3} \qquad (11)$$

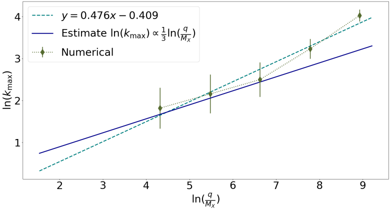

Figure: Plot of $\ln(k_{\mathrm{max}})$ against $\ln(q/M_X)$ for $q = 10^2, 10^3, 10^4, 10^5, 10^6$.

- The filled line shows the prediction (11) from Giudice et al. 1999

- The dashed line shows the linear regression of the data points with a slope of 0.476 ± 0.057

- This is not consistent with the expected scaling of $k_{\max}$ with $(q/M_X)^{1/3}$

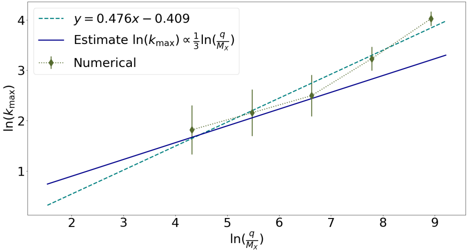

Figure: Plot of $\ln(k_{\max})$ against $\ln(q/M_X)$ for $q = 10^2, 10^3, 10^4, 10^5, 10^6$.

The estimate found in Peloso and Sorbo 2000 is

$$k_{\max} \propto \frac{q^{1/3}}{M_X^{1/6}} \sqrt{\log \frac{q^1/2}{M_X}} \quad (12)$$

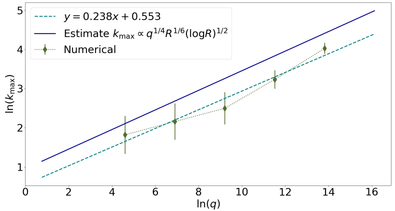

Figure: Plot of $\ln(k_{\max})$ against $\ln(q)$ for $q = 10^2, 10^3, 10^4, 10^5, 10^6$.

- The filled line shows the prediction (12) from Peloso and Sorbo 2000
- The dashed line shows the linear regression of the data points with a slope of 0.238 ± 0.028
- This is consistent with the expected scaling of $k_{\max}$ with $q^{1/4}$

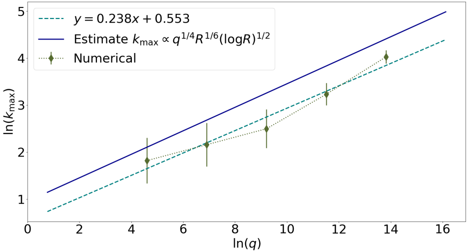

Figure: Plot of $\ln(k_{\max})$ against $\ln(q)$ for $q = 10^2, 10^3, 10^4, 10^5, 10^6$.

Estimates of the Maximum Momentum

Comparison of Results With Estimates

The estimate found in Gorbunov and Rubakov 2011 is

$$k_{\max} \simeq \left(\frac{4 m_\phi^{7/2}}{M_X^{1/2}} q \right)^{1/3} \qquad (13)$$

This estimate is in agreement with the scaling of $k_{\max}$ with respect to q and M_X in Greene and Kofman 2000

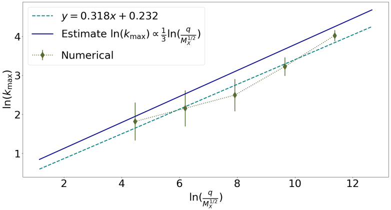

Figure: Plot of $\ln(k_{\max})$ against $\ln\left(q/M_X^{1/2}\right)$ for $q = 10^2, 10^3, 10^4, 10^5, 10^6$.

- The filled line shows the prediction (13) from Gorbunov and Rubakov 2011; Greene and Kofman 2000
- The dashed line shows the linear regression of the data points with a slope of 0.318 ± 0.038
- This is consistent with the expected scaling of $k_{\max}$ with $(q/M_X^{1/2})^{1/3}$

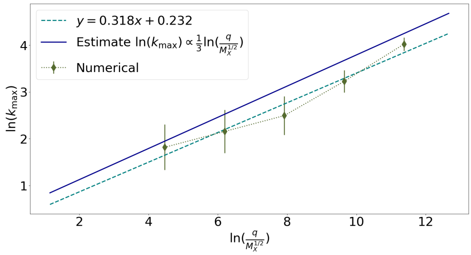

Figure: Plot of $\ln(k_{\max})$ against $\ln\left(q/M_X^{1/2}\right)$ for $q = 10^2, 10^3, 10^4, 10^5, 10^6$.